Data, Innovation, and Science Cluster

Swarm Ion Temperature Estimation: Input data and model validation

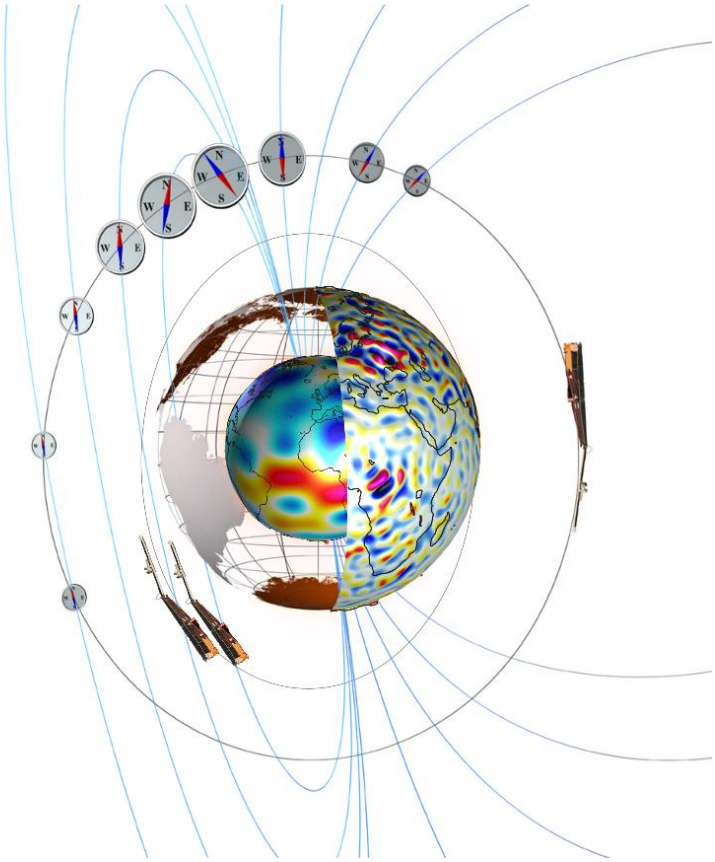

Doc. no: SW-TN-UoC-GS-002, Rev: 1, 10 Jul 2020

Prepared:

Levan Lomidze 10 Jul 2020

Project Scientist

Approved:

Johnathan Burchill 10 Jul 2020

Project Manager

Record of Changes

Reason	Description	Rev	Date
Initial vers.	Draft	1dA	8 Jul 2020
Release	Signed and released	1	10 Jul 2020

Table of Contents

Table of Figures

1 Introduction

The document provides information about validity of Swarm ion temperature model and its inputs.

1.1 Scope and applicability

This document is a deliverable of the Swarm Ion Temperature Estimation project [AD-1].

2 Applicable and Reference Documentation

2.1 Applicable Documents

The following documents are applicable to the definitions within this document.

[AD-1] SW-CO-DTU-GS-123, Rev: 1A 2019-10-08, Subcontract SITE 2.3.

2.2 Reference Documents

The following documents contain supporting and background information to be taken into account during the activities specified within this document.

[RD-1] Huba, J. D., G. Joyce, and J. Krall (2008), Three dimensional equatorial spread F modeling, Geophys. Res. Lett., 35, L10102.

[RD-2] Huba, J.D., Maute, A., and Crowley. G. (2017), SAMI3-ICON: model of the ionosphere/plasmas-phere sys-tem. Space Sci. Rev., this issue. doi:10.1007/s11214-017-0415-z

[RD-3] Picone, J. M., Hedin, A. E., Drob, D. P., & Aikin, A. C. (2002). NRLMSISE-00 empirical model of the atmos-phere: Statistical comparisons and scientific issues. Journal of Geophysical Research, 107(A12), 1468.

[RD-4] Drob, D. P., et al. (2015), An update to the Horizontal Wind Model (HWM): The quiet time thermo-sphere, Earth and Space Science, 2, doi:10.1002/2014EA000089.

[RD-5] Schunk (1996), STEP: Handbook of Ionospheric Models, Utah State Univ., Logan, Utah.

[RD-6] Huba, J.D., G. Joyce, and J.A. Fedder (2000), Sami2 is Another Model of the Ionosphere (SAMI2): A new low-latitude ionosphere model, J. Geophys. Res., 105, 23,035.

[RD-7] SW-RN-IRF-GS-005, Extended Set of Swarm Langmuir Probe Data

[RD-8] Lomidze, L., Knudsen, D. J., Burchill, J., Kouznetsov, A., & Buchert, S. C. (2018). Calibration and vali-dation of Swarm plasma densities and electron temperatures using ground-based radars and sat-ellite radio occultation measurements. Radio Science, 53.

[RD-9] SW-RN-UoC-GS-004, EFI TII Cross-Track Flow Data Release Notes

[RD-10] Weimer, D. R. (2005). Improved ionospheric electrodynamic models and application to calculating Joule heating rates. Journal of Geophysical Research, 110, A05306.

[RD-11] CIRA (2012), COSPAR International Reference Atmosphere-2012, Models of the Earth's Upper At-mos-phere, Ver1, July-31, 2012

[RD-12] Hedin, A. E., et al. (1991), Revised global model of thermosphere winds using satellite and ground-based observations, J. Geophys. Res., 96(A5), 7657–7688, doi:10.1029/91JA00251Nicolls 2006

[RD-13] Zhang, S.-R., Holt, J. M., Erickson, P. J., & Goncharenko, L. P. (2015). Day-to-day variability and solar pre-conditioning of thermospheric temperature over Millstone Hill. Journal of Geophysical Research: Space Physics, 120, 3913–3927.

[RD-14] Lomidze, L., Burchill, J. K., Knudsen, D. J., Kouznetsov, A., & Weimer, D. R. (2019). Validity study of the Swarm horizontal cross-track ion drift velocities in the high-latitude ionosphere. Earth and Space Science, 6.

2.3 Abbreviations

A list of acronyms and abbreviations used by Swarm partners can be found here. Any acronyms or abbreviations not found on the online list but used in this document can be found below.

Acronym ***or abbreviation***	***Description***
NRLMSISE	Naval Research Laboratory Mass Spectrometer and Incoherent Scatter Radar Extended
HWM	Horizontal Wind Model

3 Ion temperature model and input data validation

3.1 Outline

The Swarm ion temperature model estimates topside ionospheric ion temperature at the altitude of the Swarm satellites. The model is based on the ion energy balance equation [RD-5, RD-6]. It assumes that at low and middle latitudes the main source of the heating of the ion gas is a heat transfer from an ambient electron gas. The ion cooling occurs via collisions with neutral atoms and molecules. At high magnetic latitudes, the effects of frictional heating can be a significant heat source for ions, and are included in the model.

The model requires information about electron and neutral gases, and plasma drift. The electron density and temperature are provided by Swarm LP observations. Neutral gas composition, temperature, and winds are computed using corresponding empirical models. The ion drift velocities are obtained from Swarm TII data, and from a high-latitude empirical model to expand the temperature coverage outside the TII operations. Schematically, the ion temperature estimation concept used in the model is shown in Figure 1.

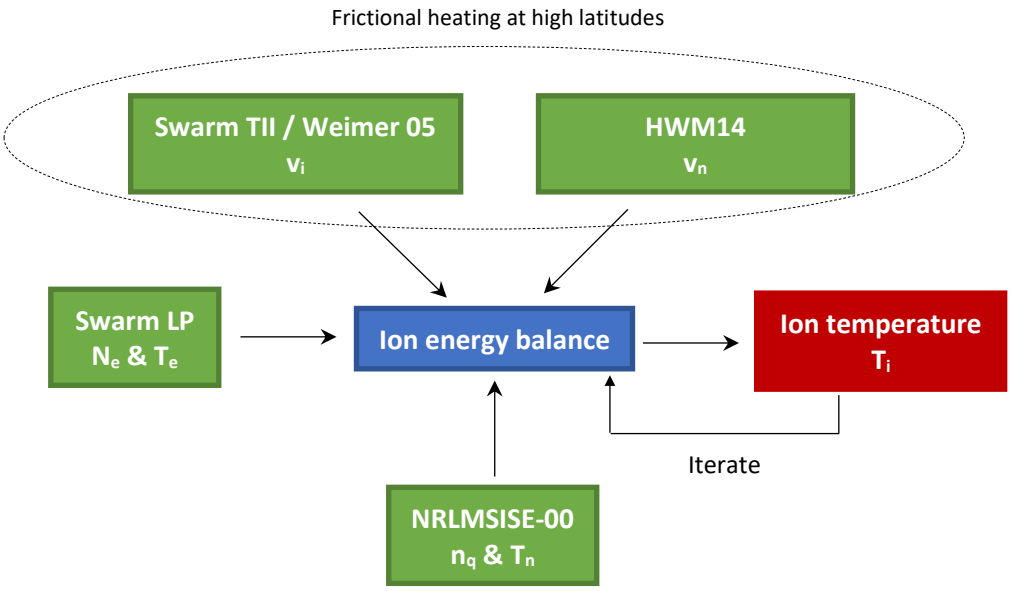

Figure 1: Schematic view of the ion temperature estimation approach.

The model errors arise due to various assumptions and uncertainties in the input data. Analysis indicates that the model accurately estimates ion temperatures at the Swarm satellites under typical ionospheric conditions. Errors (variability) in the estimated ion temperatures due to uncertainties in the input parameters are comparable to a typical precision of in-situ and remote measurements employed in space physics [e.g. RD-8 and references therein].

3.2 Model validation

3.2.1 Principle

The Swarm ion temperature model validation is accomplished using simulation results from a physics-based ionosphere model, SAMI3 (Sami3 is A Model of the Ionosphere), which was developed at the US Naval Research Laboratory [RD-1, RD-2]. SAMI3 is a global, 3-D model that self-consistently solves the continuity, momentum, and energy equations for ionospheric plasma. It includes all major physical and chemical processes, covers the altitude range between 90-20,000 km, and models evolution of seven ion species (H^+, He^+, N^+, O^+, N_2^+, O_2^+, and NO^+). The low- and middle-latitude electric fields are self-consistently solved from the potential equation. The neutral composition and temperature are specified by NRLMSISE-00 [RD-3] and winds by HWM14 [RD-4].

In SAMI3 the ion temperature is obtained from a complete heat balance equation (1), which is solved together with the equations of continuity and momentum equations of ions, and electron energy balance.

$$\frac{3}{2}k_B n_i \frac{\partial T_i}{\partial t} - \nabla \cdot (\kappa_i \nabla T_i) + \frac{3}{2}k_B n_i \mathbf{v_i} \cdot \nabla T_i + k_B n_i T_i \nabla \cdot \mathbf{v_i} = Q_{ie} + Q_{ii'} + F_{in} - L_{in} \qquad (1)$$

The Swarm ion temperature model uses a simplified version of (1) where the only terms retained in the ion temperature equation are electron-ion and ion-neutral heat transfers, and frictional heating,

$$Q_{ie} + F_{in} = L_{in} \quad (2),$$

where T_i and n_i are temperature and density of ion type "i", $\mathbf{v_i}$ is the ion velocity, Q_{ie}, $Q_{ii'}$ and L_{in} are ion heating/cooling rates due to collisions between ions and electrons, ions and ions, and ions and neutrals, respectively; and F_{in} is the ion frictional heating due to the motion of ions relative to the neutrals [RD-5, RD-6].

$$Q_{ie} = \frac{7.7\times10^{-6} n_e n_i}{A_i T_e^{1.5}}(T_e - T_i) \quad \text{eV cm}^{-3}\,\text{sec}^{-1} \; (3)$$

$$L_{in} = \sum_q \frac{3k_B n_i m_i m_q}{(m_i+m_q)^2} \nu_{iq}(T_i - T_q) \quad \text{eV cm}^{-3}\,\text{sec}^{-1} \; (4)$$

$$F_{in} = \sum_q \frac{n_i m_i m_q}{(m_i+m_q)^2} \nu_{iq} m_q (\mathbf{v}_i - \mathbf{v}_q)^2 \quad \text{eV cm}^{-3}\,\text{sec}^{-1} \; (5)$$

$$Q_{ii'} = \sum_j \frac{3.3\times10^{-4} n_i n_j}{A_i A_j (T_i/A_i + T_j/A_j)^{1.5}}(T_j - T_i) \quad \text{eV cm}^{-3}\,\text{sec}^{-1} \; (6).$$

Here q and j denote summations over neutrals and ions, respectively. $\nu_{iq} = \nu_{iq}(n_q, T_q, T_i)$ denotes ion-neutral collision frequency for energy transfer and depends on corresponding neutral density, and neutral and ion temperatures, $\mathbf{v_q}$ is the neutral wind velocity, A_i is the mass of ion "i" in atomic mass units. In the left-hand-side of equation (1) the 2nd term represents thermal conduction, the 3rd term is heat advection, and the 4th term is heat convection.

The simulated ionospheric plasma parameters from SAMI3 were used to generate electron density, and electron and ion temperature data at 460 and 520 km altitudes (the approximate altitudes of the Swarm satellites), as well as neutral gas parameters. These were then used to validate the ion temperature model (2) by comparing the true (SAMI3 calculated) and estimated (retrieved) ion temperatures.

3.2.2 Model settings

The solar and geophysical conditions for which the simulations were carried out are represent low ($F_{10.7}$=70 sfu (1 sfu (solar flux unit) = 10^{-22} W m^{-2} Hz^{-1}), medium ($F_{10.7}$=120 sfu), and high ($F_{10.7}$=170 sfu) solar activity; and quiet geomagnetic conditions (Ap=2), moderate geomagnetic activity (Ap=48) and severe (Ap=207) geomagnetic storms. In addition, the simulations where done for June and December solstices, and March and

September equinoxes to capture possible seasonal peculiarities. The grid chosen for SAMI3 simulations was (n_z, n_f, n_l) = (204, 80, 96) where n_z is the number of grid points along the geomagnetic field, n_f is the number of field lines, and n_l is the number of grid points in the longitudinal direction (longitudinal planes). The SAMI3 model data, which were generated for all universal times with 15-minute resolution, were interpolated to a 2°×7.5°×10 km (Glat×Glon×Alt) uniform grid between -79° - 79° Glat, -176.25° - 176.25° Glon, and 90 - 800 km. To study the model validity at high latitudes the latitudinal grid was extended to ±90° to better cover the high latitude part of the ionosphere.

Figure 2 shows typical altitude profiles of electron, ion (O^+), and neutral temperatures (middle latitudes, daytime), and magnetic latitude-local time distributions of O^+ ion density, electron temperature, and ion temperature at 460 km during March equinox for medium solar flux and quiet conditions. The two dashed lines in Figure 2a indicate approximate altitudes of Swarm A/C and Swarm B satellites. The ion temperature usually has an intermediate value between the electron and ion gases in the ionosphere that increases with altitude. The ion gas is hotter during day than at night, and is hotter at middle and high latitudes than at low latitudes.

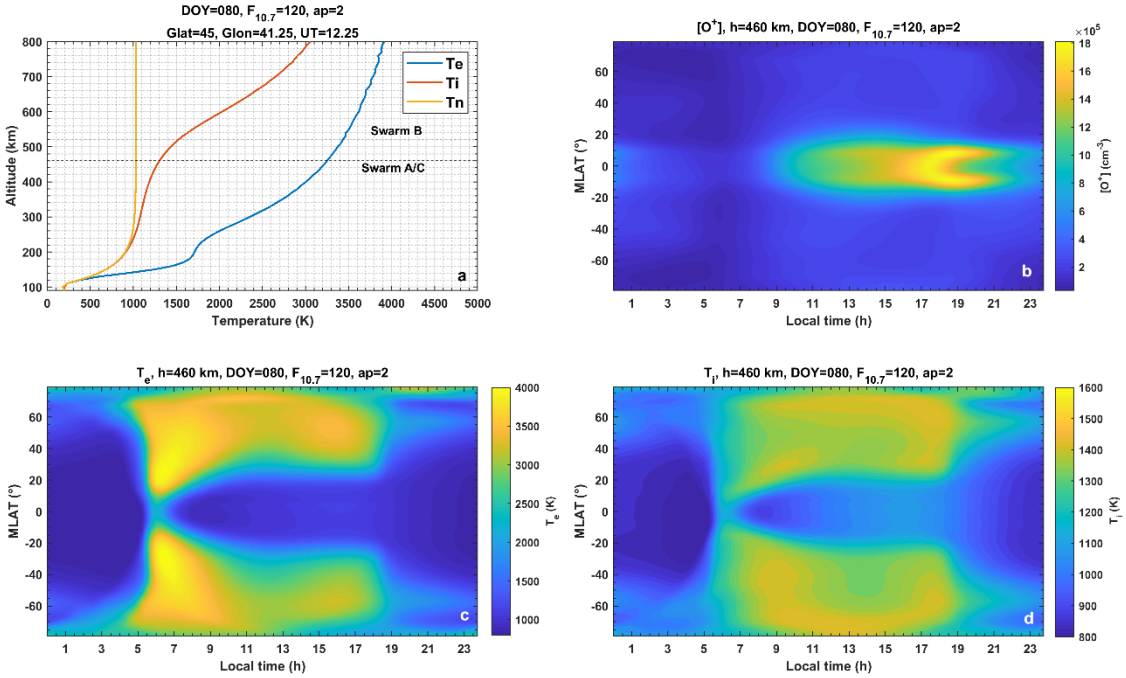

Figure 2: (a) Altitude profiles of middle latitude electron, ion, and neutral temperatures, and magnetic latitude-local time distributions of (b) O^+ ion density (≈n_e), (c) electron temperature, and (d) ion (O^+) temperature. The results correspond to March equinox, medium solar flux, and quiet geomagnetic conditions.

3.2.3 Model error dependence on geophysical conditions

The synthetic (i.e. SAMI3 model generated) data of n_i and T_e (as well as neutral composition and temperature) were used to estimate ionospheric ion temperature (T_i) at 460 km and 520 km altitudes based on simplified heat balance equation (2) at low and middle latitudes with the assumption of $F_{in} = 0$. The role of frictional heating, F_{in}, is strong at high geomagnetic latitudes, and error in T_i due to uncertainty in ion drift velocity were estimated separately (Section 3.2.5). Note that even though the SAMI3 results extend to high latitudes, the version of the model used in this report omits the high-latitude convection electric field.

In order to be consistent with Swarm LP observations, the n_i was assumed to be equal to the density of O^+ ions and n_i=n_e. Initially, T_i was assumed to be the same as T_n, then the equation (2) was iterated until the difference between the two consecutive estimates was less than 1 K.

To investigate limitations of this approach to estimating ion temperature, the difference between the estimated (2) and true (1) ion temperatures (($T_{est.}$-T_{true})/T_{true} x 100 %) was calculated for different solar and geophysical conditions. Since the major variation of ionospheric parameters (in addition to solar flux, season, and geomagnetic activity) occurs with latitude and local time, the differences are generated for zonally averaged ion temperatures at 460 km and 520 km altitudes (Figure 3 and 4).

The results indicate that the simplified ion heat balance equation has sufficiently high accuracy (< 5% for 460 km, 5-10 % for 520 km) for the majority of cases presented in Figure 3 and 4. The error is largest in the winter hemisphere for low solar flux conditions, for which this technique may underestimate ion temperatures by up to 50 %. The summer hemisphere and equinox season (both hemispheres) show that the technique may underestimates ion temperatures by 10-25 % during low solar flux. The error tends to be the largest during morning and evening hours, and at middle and high latitudes. Generally, the accuracy is better for lower altitude (460 km), which implies that the accuracy of estimated ion temperatures should be about 5-10 % better for Swarm A/C than for Swarm B. For the disturbed geomagnetic conditions, the errors are only noticeable at high latitudes, however at high latitudes the error in frictional heating term can introduce additional error (Section 3.2.5).

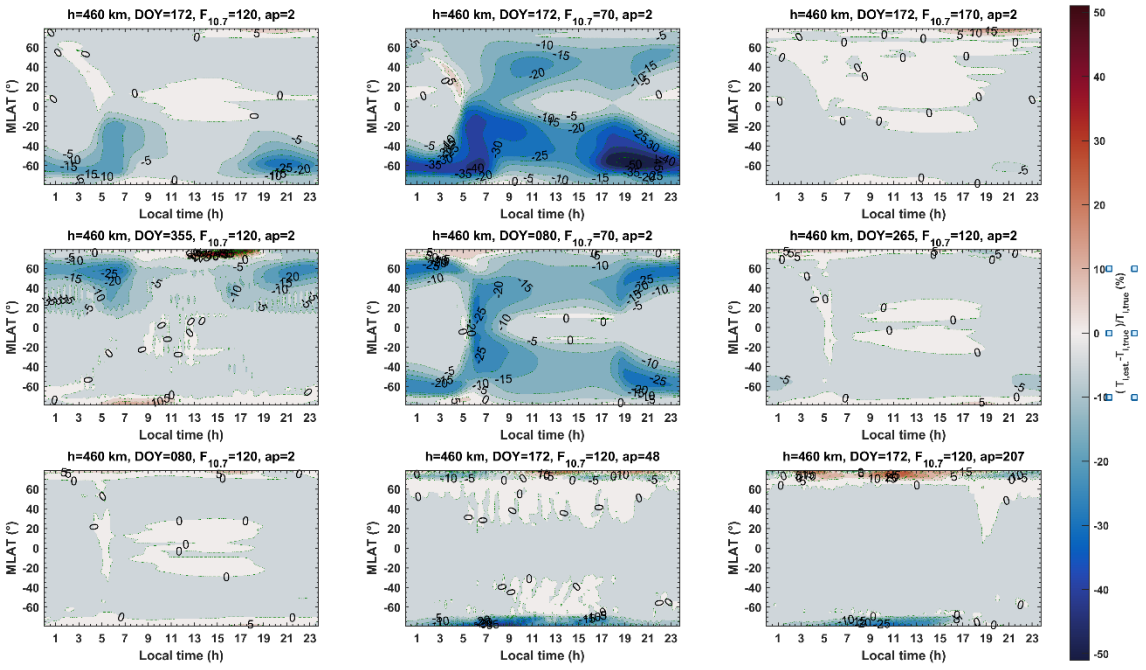

Figure 3: Differences (in %) between the estimated and true ion temperatures at 460 km as a function of magnetic latitude and local time for different seasons, and solar and geomagnetic conditions.

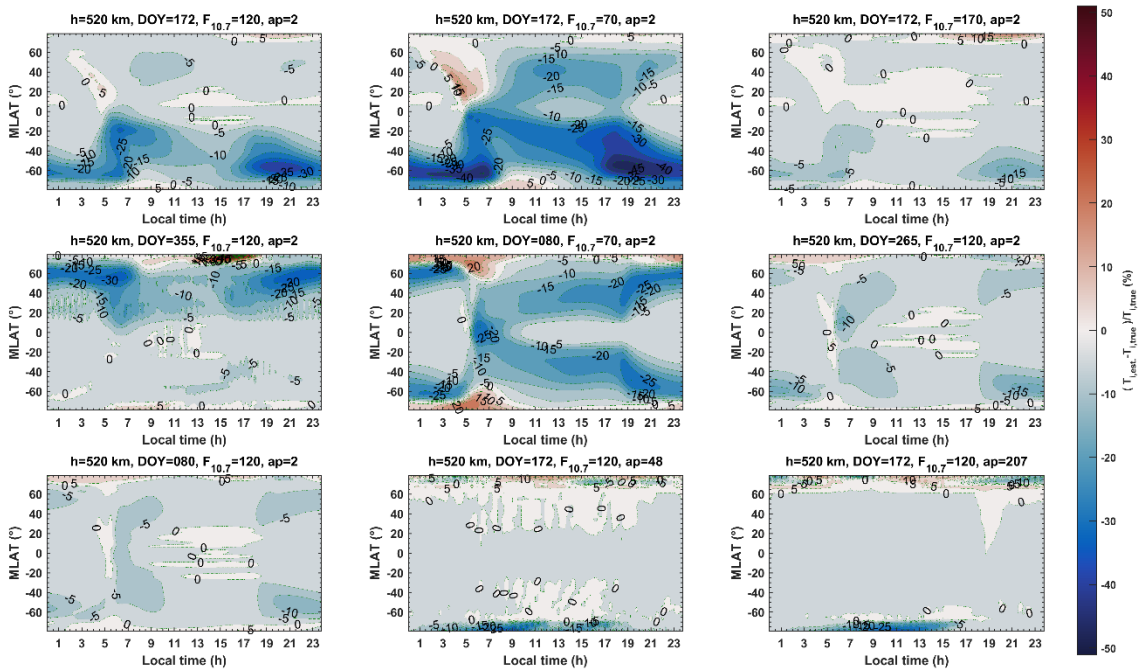

Figure 4: Same as Figure 3, but for 520 km altitude.

3.2.4 Light ion effects

In the topside ionosphere at the altitude of the Swarm satellites, besides the major O^+ ions, the minor light ions, such as H^+ and He^+, are also present. Their concentration however can become significant at solar minimum during nighttime. The different ion species have different temperatures, with light ions typically having higher temperatures.

Figure 5 shows altitude profiles of O^+, H^+, and He^+ densities and temperatures obtained using the SAMI3 model for the case of low solar flux ($F_{10.7}$=70) and December solstice at middle-latitude locations during early morning (UT=3.5 h, LT=6.25 h). The two dashed lines indicate the altitudes of the Swarm A/C (~460 km) and Swarm B (~520 km) satellites. In line with observations, in the given example the transition height (altitude at which O^+ density is equal to that of light ions) is below 600 km, and the light ion temperatures exceed that of O^+ by few hundred Kelvin. Note that with increasing altitude, O^+ gradually becomes the minor ion species.

The ion-ion heat exchange term, which is given by equation (6), is omitted from the Swarm ion temperature model. The reason for the omission is that for Swarm mission neither light ion densities, nor their temperature measurements are available. Nevertheless, it is important to understand the temperature error caused by this approximation.

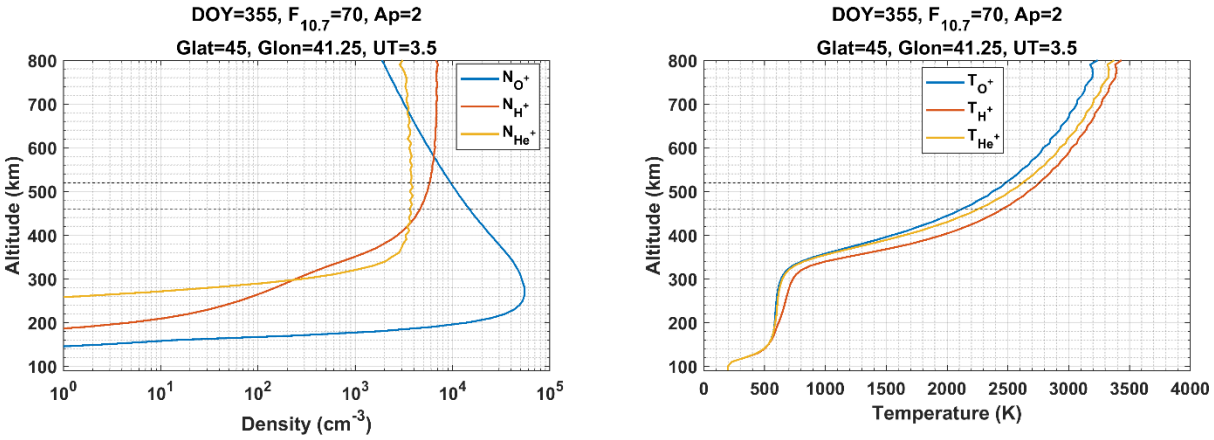

Figure 5: (Left) Altitude profiles of middle latitude O^+, H^+, and H^+ densities, and (right) corresponding temperatures. The results correspond to December solstice, low solar flux, and quiet geomagnetic conditions.

Figure 6 shows the SAMI3 ion temperatures (O^+ ion temperatures) calculated using the full heat balance equation. As in previous figures, for the subsequent cases they are considered as 'true' temperatures to which the retrieved temperatures are compared. Note the hemispheric asymmetry of the temperature during solstices, the symmetry during equinox, and also higher temperature at 520 km compared to 460 km – all of which are expected to be present in both observational and properly modelled data.

The O^+ ion temperature was then estimated using SAMI3 model-generated inputs and ion heat balance (2), now including two cases: with and without the $Q_{ii'}$ term. Because the effect of light ions is expected to be more important during low solar flux, results for only low solar activity condition are shown.

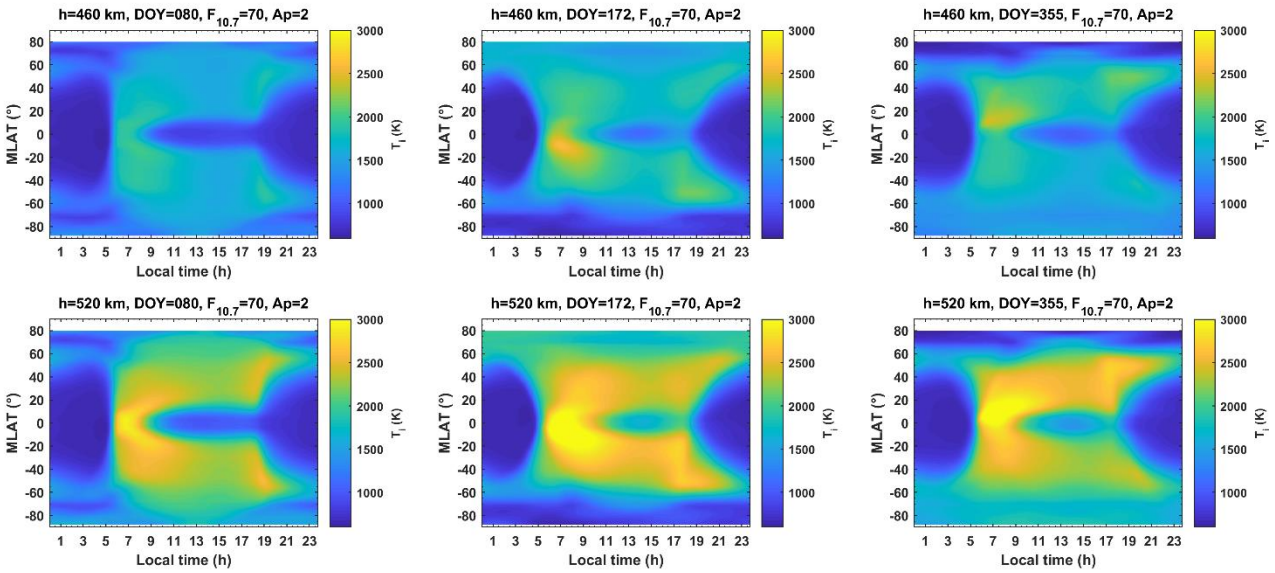

Figure 6: Magnetic latitude - local time variation of SAMI3 ion temperature ($T_{i,true}$) at 460 km and 520 km for three different seasons, during low solar flux and quiet geomagnetic conditions.

The top rows in Figures 7 and 8 compare the difference (in %) between the estimated and true ion temperatures ($(T_{est.}-T_{true})/T_{true}$) when the ion-ion heat exchange term is ignored for Swarm A/C and Swarm B altitudes,

respectively. These represent the conditions for which the underestimation can be largest (~50%, winter hemisphere, morning/evening hours, also see Figure 3 and 4). The bottom rows in Figures 7 and 8 also compare the true ion temperature to the estimated one, but with the heat exchange term between O^+ and light ions included in the estimate.

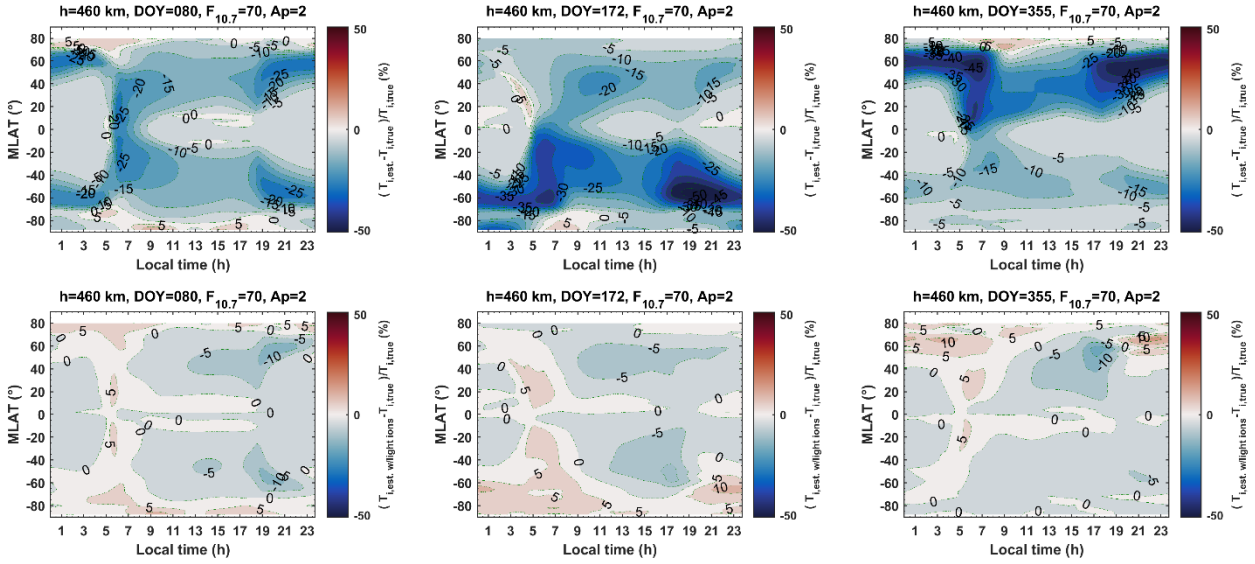

Figure 7: Differences (in %) between the estimated and true ion temperatures at 460 km as a function of magnetic latitude and local time for different seasons, low solar flux, and quiet geomagnetic conditions. Top row is without the light ion (H^+, He^+) effects in the heat equation, and bottom row is with the ion-ion heat exchange between O^+ and them.

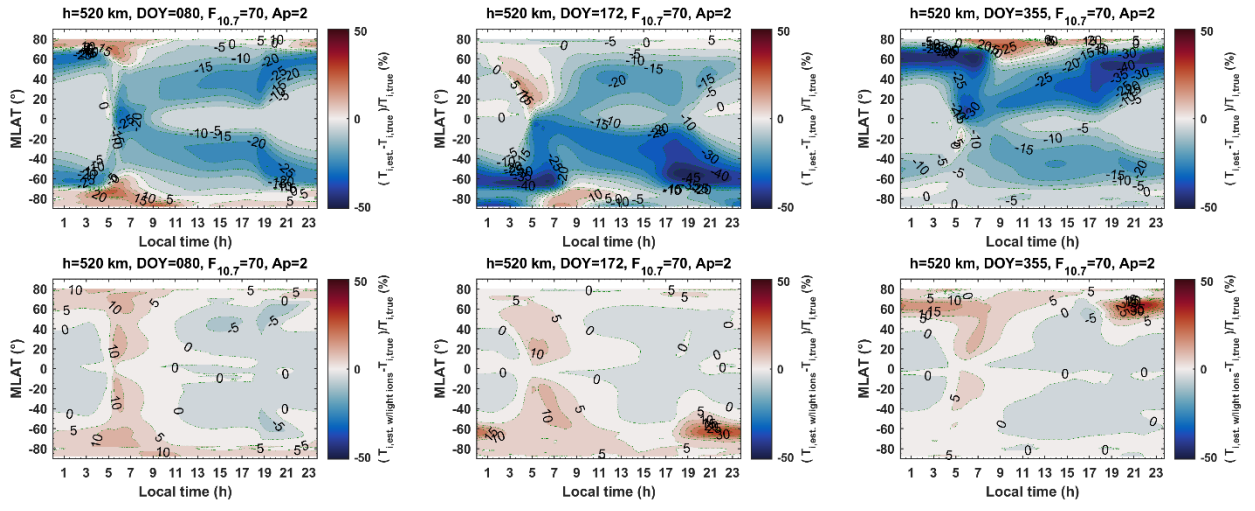

Figure 8: Same as Figure 7, but for 520 km altitude.

These results demonstrate that the inclusion of the ion-ion heat exchange term significantly improves the ion temperature retrieval accuracy. For the most part the error is around 5-10 %. The overestimation is most evident generally during morning hours, and additionally in the winter hemisphere during evening hours. The underestimation is more widespread during daytime but is smaller in magnitude. Because the light ions are

usually expected to have higher temperatures than O^+, they act as a heat source for it. This explains the relatively large underestimation of ion temperature by the ion temperature model when the presence of light ions are significant but ignored (during morning/evening and winter hemisphere).

The results (bottom rows in Figure 7 and 8) also show that the temperature accuracy under the presence of light ions is better for Swarm A/C altitudes than for Swarm B. For Swarm B the overestimation for the winter hemisphere during a few hours in late evening can be 30-40%, whereas it is 10-15 % for Swarm A/C. The increase in the relative proportion of light ions with altitude, and the increase of the relative role of heat sinks related to thermal conduction, heat advection, and heat conduction, which are omitted, is a plausible explanation of both temperature overestimation and its altitude dependence for the cases when the light ions considered. The results are important for understanding the sources of errors in the ion temperature model. Furthermore. it potentially leaves room for future improvements, highlighting the importance of the estimation or measurements of light ion parameters the topside ionosphere.

3.2.5 Uncertainty due to the errors in high-latitude frictional heating

At high latitudes, poleward of about 60° magnetic, the ion frictional heating needs to be taken into account in the ion temperature model. The corresponding term is given by equation (5). In the Swarm ion temperature model, the ion velocity is taken either from Swarm TII observations or the Weimer 2005 model, and the neutral wind velocity is provided by the HWM14 empirical wind model. Errors in ion and neutral velocities are expected to affect the frictional heating term, and thus the estimated ion temperatures.

To estimate how the high-latitude ion and neutral flow velocity errors translate into the estimated ion temperature uncertainty at high-latitudes, the temperature error estimation was performed by assuming four different constant values of the magnitude of the error δv (δv is the error due to uncertainties in both ion drift and neutral winds): 100, 400, 700, and 1000 m/s. The results for medium solar activity and June solstice are given In Figure 9 and 10, respectively. Shown are the fractional differences (in %) between the estimates of ion temperatures with no frictional heating error (δv=0 m/s) and those with four different δv values. In all cases $|\mathbf{v}_i - \mathbf{v}_q|$ = 500 m/s is assumed, which corresponds to significant frictional ion heating.

Figures 9 and 10 show the error distributions as a function of magnetic latitude and local time during medium solar activity and June solstice case for Swarm A/C and Swarm B altitudes, respectively.

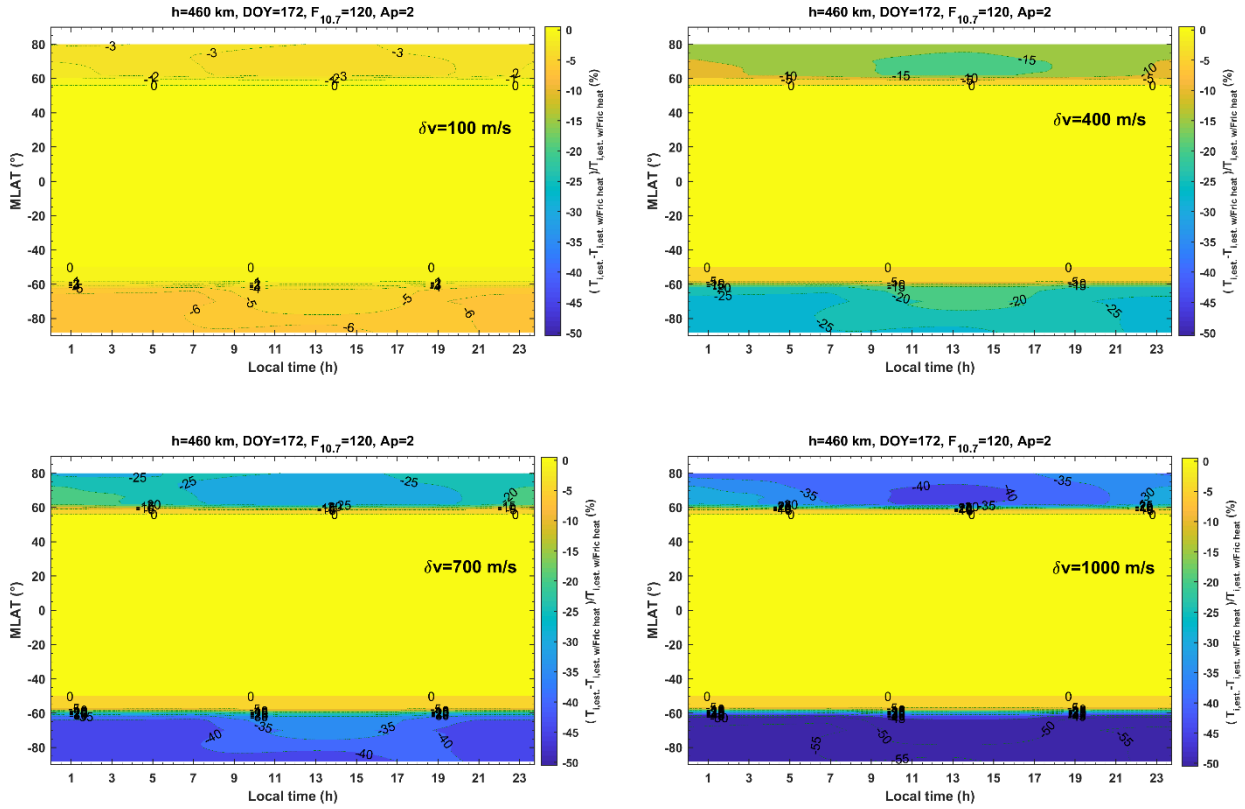

Figure 9: Magnetic latitude-local time variation of ion temperature errors in high latitudes for four different values of relative ion drift velocity errors (δv). The cases are for 460 km, June solstice and medium solar activity.

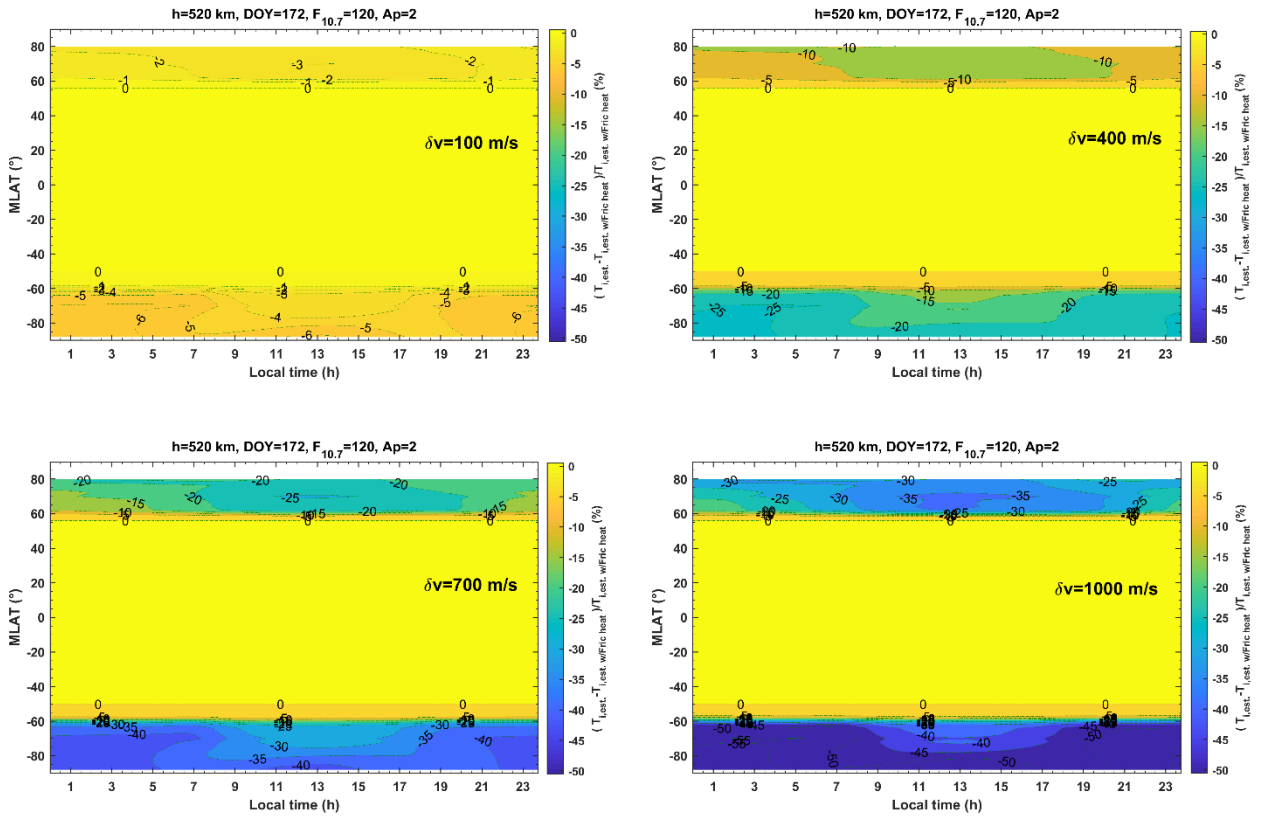

Figure 10: Same as Figure 9, but for 520 km altitude.

The temperature error is zero at low and middle latitudes because of the frictional heating term is taken into account only at high latitudes. These estimates show that the error in the ion temperature due to the uncertainty in high-latitude drifts and winds, when significant, is expected to range between 15-40 %. The errors appear to be larger in the winter polar ionosphere (20-40 %), compared to those in the summer one (15-25 %). Where lower limits correspond to δv=400 m/s and upper limits to δv=700 m/s. For smaller error (δv=100 m/s) the temperature uncertainty is only as high as 6 %. Moreover, the errors appear to be about 5 % smaller for Swarm B altitude. This is consistent with the relatively less dense ionosphere and thermosphere at higher altitude, resulting in less frictional heating.

Note that the assumed 500 m/s magnitude of the difference between ion and neutral velocities corresponds to strong frictional heating, and uncertainties of the order of 500 m/s error also corresponds cases with significantly erroneous wind and drift values. It is reasonable to expect that many of the Swarm orbits will have smaller relative drift and wind errors. Overall, this error analysis indicates that the ion temperature uncertainty due to errors in ion frictional term is comparable or smaller than that due to the omission of light ion effects from the temperature model.

It should also be noted that, in contrast with the light ion effects, the frictional heating term errors do not show noticeable variation with solar flux. Therefore the presented cases in Figures 9 and 10 are for medium solar activity conditions ($F_{10.7}$=120). The solstice case was chosen to highlight seasonal differences. The equinox case (not shown) exhibited errors ranging between the summer and winter values.

3.2.6 Effects of input data quality/error on the estimated ion temperature

The ion temperature estimation above assumes that all ionospheric and thermospheric inputs are precisely known. However, the analysis shows (Section 3.3) that the one-sigma random error in Swarm LP measurements of N_e and (high-gain LP) T_e after their bias corrections are about 16 % and 200 K, respectively. In addition, the typical errors associated with NRLMSISE-00 neutral density and temperature are 15-20 % and 50 K, respectively. The errors are also associated with drifts from Swarm TII and Weimer 2005 model drifts, and with neutral winds from HWM14, whose effects were discussed in previous section.

In order to understand the effects of these errors in input data on the estimated ion temperatures, each model input at given location (Glat, Glon, Alt) and time was modified by adding to it a sequence of 1000 random values with zero mean and with standard deviation equal to their typical value of standard error σ. Then, for each of these values the standard deviation of estimated ion temperature was computed. The process was repeated for all locations and solar/geophysical conditions and MLAT-LT maps were generated (Figure 11 and 12).

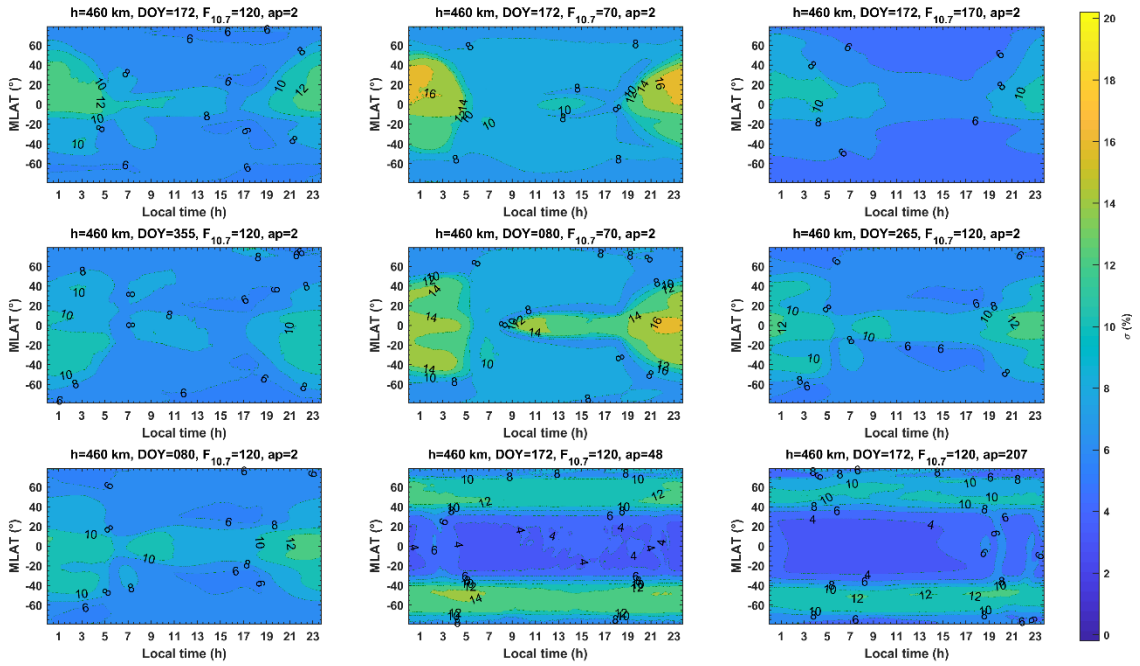

Figure 11: Magnetic latitude - local time variation of relative error σ (in %) at 460 km of estimated ion temperature due to typical errors in the ion density, electron temperature, neutral density, and neutral temperature.

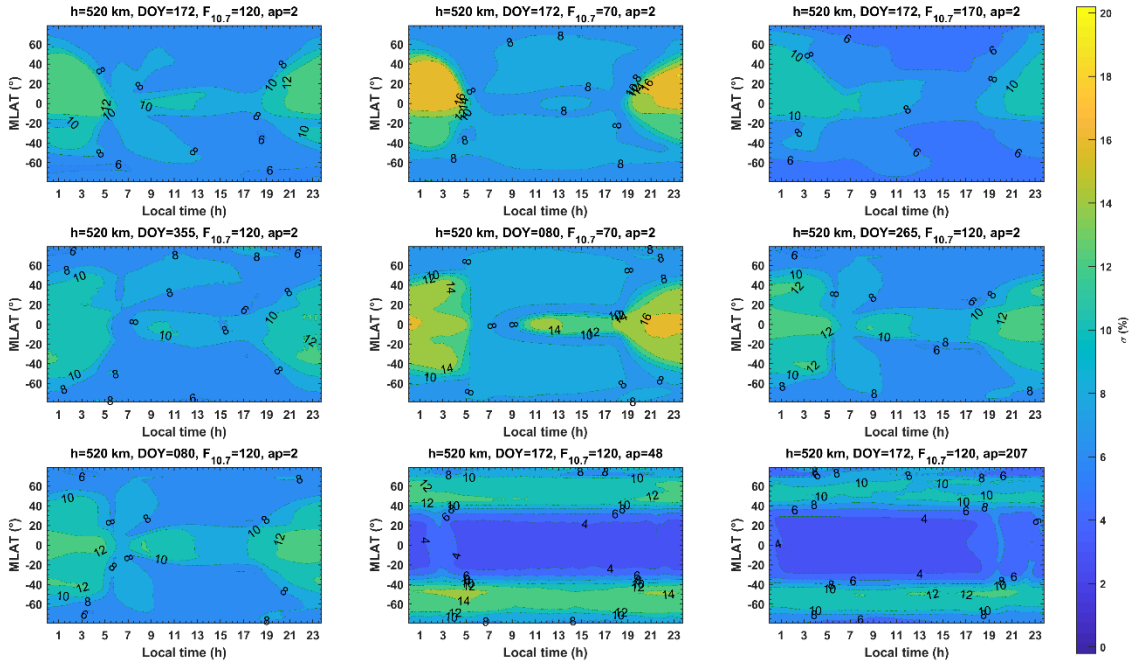

Figure 12: Same as Figure 11 but for 520 km altitude.

These results show that the cumulative effect of typical errors of inputs (associated with the Swarm LP ion density, electron temperature, and NRLMSISE-00 neutral density and neutral temperature) is a random deviation of estimated ion temperature from its 'precise input-based' value by about 3-17 %. Note that in both

precise and modified cases equation (2) was used. The figures show that there is no significant difference between the two altitudes (460 km and 520 km). During quiet times the error is slightly larger (10-15 %) at equatorial and low latitudes than at middle latitudes (5-8 %), but this larger error expands towards middle latitudes between evening and morning interval. For geomagnetically disturbed conditions the low and middle latitude σs are around 4 % and become 10-14 % at high latitudes.

3.3 Validity of model inputs

The ion temperature model inputs consist of corrected Swarm LP observations of electron density and temperature [RD-7, RD-8], and neutral composition and temperature, which are calculated using NRLMSISE-00 model [RD-3]. At high magnetic latitudes (≥60°) the ion frictional heating term is also included. The horizontal components of neutral wind velocity are computed using HWM14 empirical wind model [RD-4]. The high-latitude ion drifts are calculated for two cases: one based on Swarm TII measurements [RD-9], and the other based on the Weimer 2005 empirical convection electric field model [RD-10].

The calibration and validation of Swarm LP electron densities and temperatures have been performed in RD-8 by using data from nearly coincident measurements from low- and middle-latitude incoherent scatter radars, low-latitude ionosondes, and Constellation Observing System for Meteorology, Ionosphere, and Climate (COSMIC) satellites. It was found that initially the Swarm LPs systematically underestimate plasma frequency ($\propto \sqrt{n_e}$) by about 10% (0.5–0.6 MHz). However, the correlation coefficients were high (≥0.97), indicating accurate relative variation in the Swarm LP densities. The comparison of T_e from high-gain LPs and those from ISRs revealed that all three satellites overestimate it by 300–400 K but exhibit high correlations (0.92–0.97) against the validation data. The low-gain LP T_e data showed larger overestimation (~700 K) and lower correlation (0.86–0.90).

The adjustment of the Swarm LP data based on Swarm-ISR comparison results removed the systematic errors in the Swarm data and provided plasma frequencies and high- and low-gain electron temperatures that are precise to within about 0.4 MHz (8%), 150–230 K, and 260–360 K, respectively. The Swarm LP n_e and T_e calibration and validation work included only low and middle latitude ISRs, and covered the date range between December 2013 and June 2016. Re-evaluation of the Swarm LP data calibration and validation is planned by extending the time interval to newer (up to date) Swarm LP data and by including high-latitude ISR data. The LP data will also be corrected accordingly.

The NRLMISISE-00 model provides the neutral species' temperatures and densities in the upper atmosphere. The model is based on a very large set of data from space- and ground-based measurements with extensive temporal and spatial distribution for a wide range of geophysical conditions [RD-3, RD-11]. The model has been extensively tested against experimental data and is used in many applications by the space science community, including ionospheric data assimilation models. For mean activity conditions, the estimated uncertainty of the NRLMSISE-00 species density is 15–20 %, but for short term and local-scale variations, the estimated uncertainties are significantly larger [RD-11, RD-12]. The characteristic error in neutral temperature can be up to ~50 K [RD-13, RD-14]. The NRLMSISE-00 model provides statistical averages including information about the average upper-atmospheric state under geomagnetic storm conditions. However, at high latitudes and high geomagnetic activity, because of limited data, the model does not capture well the local structure and shorter timescales associated with any particular storm [RD-3].

A study of the validity of Swarm A and Swarm B EFI TII 2Hz horizontal cross-track ion drift velocities in the high-latitude ionosphere was performed in RD-15 by examining the climatology of high-latitude ion convection under different interplanetary magnetic field (IMF) and solar wind conditions. After a recalibration of the drifts using a refinement of the baseline offset removal, the cross-track ion drift climatology was found to

properly correspond to the changing geospace environment and to agree reasonably well statistically with the Weimer 2005 empirical convection electric field model. Overall (both hemispheres, all IMF conditions), the agreement was statistically within about 200 m/s and the correlation coefficient was 0.73, with the corresponding magnitudes of Swarm A and Swarm B drifts ~34% and ~51% larger than the model estimates, respectively. The best correspondence, however was obtained for Swarm-A in the northern hemisphere during the southward IMF, which showed the measured drifts larger only by 14% and correlations of 0.84. No significant systematic errors were found in the revised Swarm horizontal cross-track drift velocities. Swarm C TII operations have been limited to one science orbit and its data appear more strongly affected by the imaging anomaly. The along-track and vertical drifts have not been validated. Preliminary analysis of the newly released 0301 version of Swarm TII ion cross-track drift data [RD-9] shows noticeable improvements in the agreement with Weimer 2005 model. Random errors for the individual Swarm TII measurements are estimated from noise levels in the flows at mid-latitude.

The primary output of the Weimer 2005 empirical electric potential model is an electric field potential in the polar ionosphere at a given altitude, including the altitude of Swarm, for arbitrary IMF, solar wind, and dipole tilt angle conditions, as a function geomagnetic latitude and magnetic local time [RD-10]. The model also provides eastward and northward components of the electric field, which are used to calculate the ion drift velocity in the frictional heating term. Weimer 2005 includes a nonlinear response to the IMF magnitude, a dependence on the auroral electrojet *AL* index, as well as an improved representation of a low-latitude boundary of the electric field. The comparison of the Weimer 2005 results with corresponding measurements from the DMSP satellites showed good agreement [RD-10]. Known limitations of the model are its inability to properly respond to large-magnitude and sudden changes in the solar wind dynamic pressure and a lack of accounting for penetration electric fields at subauroral latitudes during major geomagnetic storms [RD-10]. Overall, the model is considered sufficiently robust in a statistical sense to specify the high-latitude ion drifts.

At high-latitudes the thermospheric neutral winds required for the ion temperature model are calculated using empirical Horizontal Wind Model HWM14 [RD-4] along the Swarm orbits. The model is based on a wind database from various satellite- and ground-based measurements, and provides climatological average zonal and meridional components of the neutral wind as a function of latitude, longitude, altitude, day of year, time of day, and magnetic activity. The latest update improves global specification of the upper atmospheric general circulation patterns and migrating tides, which are self-consistent with climatological ionosphere plasma distribution and electric field patterns. One of the limitations of the model includes its currently unavailable solar activity dependence [RD-4]. This effect is expected to be significant only at night. There is also difficulty in representing high-latitude circulation in geographic coordinates during winter when few satellite-based measurements are available. On the whole, HWM14 is expected to provide the reasonable estimates of the neutral motions at high-latitudes along the Swarm orbits.